Early Version – Uncorrected



Liposomal Delivery of Mangosteen Pericarp Extracts for Enhanced Anti-Aging Activity

Suwipa Ungphaiboon, Ph.D., Jirawan Jantaboon, M.Sc., Chatchai Wattanapiromsakul, Ph.D., Duangkhae Maneenuan, B.Sc., Niwan Tanmanee, M.Sc.

DOI: http://dx.doi.org/10.31584/jhsmr.20261501

Received: 6 May 2026

Revised: 11 May 2026

Accepted: 13 May 2026

Published online: 9 November 2026

This paper was from The 8th Current Drug Development International Conference 2026 (May 21-23, 2026).

Please cite this article as: Ungphaiboon S, Jantaboon J, Wattanapiromsakul C, Maneenuan D, Tanmanee N. Liposomal delivery of mangosteen pericarp extracts for enhanced anti-aging activity. J Health Sci Med Res 2026. doi: http://dx.doi.org/10.31584/jhsmr.20261501

Early Version — Uncorrected: This accepted manuscript has not been typeset or proofread. Content and formatting may change prior to final publication and should not be regarded as the final Version of Record.

© 2026 JHSMR. Hosted by Prince of Songkla University.

This is an open access article under the CC BY-NC-ND license (https://creativecommons.org/licenses/by-nc-nd/4.0/).

Original Article

Liposomal delivery of mangosteen pericarp extracts for enhanced anti-aging activity

Suwipa Ungphaiboon, Ph.D.[1*], Jirawan Jantaboon, M.Sc.[1], Chatchai Wattanapiromsakul, Ph.D.[2], Duangkhae Maneenuan, B.Sc.[1], Niwan Tanmanee, M.Sc.[3]

[1]Drug Delivery System Excellence Center, Department of Pharmaceutical Technology, Faculty of Pharmaceutical Sciences, Prince of Songkla University, Hat Yai, Songkhla 90110, Thailand.
[2]Department of Pharmacognosy and Pharmaceutical Botany, Faculty of Pharmaceutical Sciences, Prince of Songkla University, Hat Yai, Songkhla 90110, Thailand.
[3]Pharmaceutical Laboratory Service Center, Faculty of Pharmaceutical Sciences, Prince of Songkla University, Hat Yai, Songkhla 90110, Thailand.

*Corresponding Author

Contact: Suwipa Ungphaiboon

Affiliation: Department of Pharmaceutical Technology, Faculty of Pharmaceutical Sciences, Prince of Songkla University, Hat Yai, Songkhla 90110, Thailand.

E-mail: suwipa.u@psu.ac.th

ORCID iD: 0000-0001-5980-9312

Running Title: Liposomal Mangosteen for Anti-Aging

Early Version - Uncorrected

Abstract:

Objective: This study aimed to characterize bioactive compounds in mangosteen (*Garcinia mangostana* L.) pericarp extracts, evaluate their anti-aging–related biological activities, and investigate the potential of liposomal delivery systems for topical applications.

Materials and Methods: Crude ethanolic extract and α-mangostin-rich extract were prepared and analyzed for α-mangostin content, total phenolics, and tannins. In vitro antioxidant, anti-tyrosinase, and sunscreen activities were assessed. Liposomal formulations containing the selected extract were prepared and characterized for particle size, polydispersity index (PDI), zeta potential, and entrapment efficiency. The optimized formulation was incorporated into a lotion base and evaluated for anti-aging activity.

Results: The crude extract (17.8% α-mangostin) and α-mangostin-rich extract (78.7% α-mangostin) exhibited distinct activity profiles. The α-mangostin-rich extract showed stronger tyrosinase inhibition and greater sunscreen activity but lower antioxidant capacity compared to the crude extract. The optimized liposomal formulation, composed of α-mangostin-rich extract, phosphatidylcholine, and Tween 80 (1:3:0.6, w/w), produced vesicles with a mean particle size of 306.83 ± 1.50 nm, PDI of 0.27 ± 0.01, zeta potential of −38.50 ± 2.49 mV, and entrapment efficiency of 77.6 ± 0.1%. Incorporation of extract-loaded liposomes into lotion significantly enhanced anti-tyrosinase and sunscreen activities compared with the non-encapsulated extract.

Conclusion: α-Mangostin–rich extract demonstrates promising multifunctional anti-aging properties. Liposomal encapsulation improves physicochemical properties and biological activities, supporting its potential application in advanced cosmeceutical formulations.

Keywords: Anti-aging, liposomes, mangosteen pericarp

Introduction

Skin aging is a multifactorial biological process influenced by intrinsic factors such as genetic and hormonal influences, as well as extrinsic factors, particularly ultraviolet (UV) radiation[1]. Among environmental stressors, solar UV radiation is the principal contributor to premature skin aging (photoaging), largely through the generation of reactive oxygen species that

Early Version - Uncorrected

degrade collagen and disrupt extracellular matrix integrity. These oxidative processes impair skin elasticity, promote wrinkle formation and dyspigmentation, and accelerate the molecular damage of deoxyribonucleic acid, proteins, and lipids, contributing to age-related degenerative changes.

Mangosteen (*Garcinia mangostana* L.) pericarp extract has gained significant attention in cosmetic and dermatological research due to its diverse bioactivities, including anti-acne, anti-inflammatory, antioxidant, skin-whitening, and photoprotective activities, largely attributed to α-mangostin and phenolic constituents[2–5]. Importantly, the yield and composition of bioactive constituents in mangosteen pericarp extract are significantly affected by the extraction methodology. Different solvent concentrations significantly influence extract composition; for instance, 50% ethanol yields phenolic and tannin-rich extracts associated with strong radical-scavenging activity, whereas 95% ethanol produces α-mangostin-rich extracts associated with anti-acne effects[6]. Despite its widespread commercial use, comprehensive evaluation of its anti-tyrosinase activity and sunscreen potential remains limited, and systematic optimization of extraction strategies for anti-aging applications has yet to be established.

In addition to bioactive composition, the delivery system plays a critical role in determining therapeutic and cosmetic efficacy. Liposomes are widely used in dermatological formulations because their lipid bilayer structure mimics stratum corneum lipids, thereby enhancing dermal penetration and improving skin hydration and barrier function[7]. Beyond serving as carriers, liposomes have been shown to enhance collagen retention and modulate inflammatory and matrix-degrading markers in UV-damaged skin models without cytotoxicity[8,9]. Taken together, these advantages make liposomes highly promising carriers for improving the dermal delivery and activity of plant-derived bioactive compounds.

To date, investigations have predominantly addressed either extraction-driven variations in mangosteen phytochemicals and their bioactivities or the role of liposomal systems in enhancing skin delivery. In contrast, the combined optimization of extraction processes and delivery platforms for anti-aging applications remains insufficiently studied, particularly regarding anti-tyrosinase and photoprotective effects. Based on these considerations, this study aimed to optimize the extraction of mangosteen pericarp to obtain bioactive compounds-rich extracts with potent anti-aging activity and to develop liposomal formulations to enhance their physicochemical properties and biological activities.

Early Version - Uncorrected

Materials and Methods

Material

α-Mangostin (96.5 % purity) was obtained from Chromadex™ (California, USA). Folin-Ciocalteu's phenol reagent and gallic acid were purchased from Merck (Darmstadt, Germany). Kojic acid was obtained from Hangzhou Reb Technology Co., Ltd. (Hangzhou, China). L(+)-Ascorbic acid was purchased from Poch S.A. (Gliwice, Poland). Chitosan (low molecular weight), dimethylsulfoxide (DMSO), L-3,4-dihydroxyphenylalanine (L-DOPA), 2, 2-diphenyl-1-picrylhydrazyl (DPPH), mushroom tyrosinase enzyme, and L-phosphatidylcholine from soybean (Type II-S) were purchased from Sigma-Aldrich (Missouri, USA). Tannic acid was obtained from Fluka Chemika (Buchs, Switzerland). Polyvinyl-polypyrrolidone (PVPP), Polyoxyethylene (80) sorbitan monooleate (Tween 80), and propylene glycol were obtained from P.C. Drug Center Co., Ltd. (Bangkok, Thailand). Sepigel® 305 [Polyacrylamide (and) C13-14 isoparaffin (and) laureth-7] was purchased from Adinop Co., Ltd. (Bangkok, Thailand). All chemicals were used as received.

Plant materials

Fresh mangosteen (*Garcinia mangostana* L.) fruits with a dark reddish-purple pericarp, cultivated in Chumphon Province, Thailand, were obtained from a local fresh market in Hat Yai, Songkhla Province, Thailand. The plant material was authenticated, and a voucher specimen (No. SKP 0803071301) was deposited at the Herbarium of the Faculty of Pharmaceutical Sciences, Prince of Songkla University, Hat Yai, Songkhla, Thailand.

Mangosteen pericarp extracts and bioactive compound analysis

Dried mangosteen pericarp powder (4 kg) was macerated in 95% (v/v) ethanol (6 L) for 7 days. The extraction was repeated three times, and the resulting extracts were combined to yield the crude mangosteen pericarp extract. To obtain an α-mangostin-rich extract, the crude ethanolic extract was subjected to silica gel column chromatography (5 × 30 cm) using petroleum ether:ethyl acetate (7:3, v/v) as the mobile phase, following the method described by Amnuaikit et al. (2012)[2].

High-performance liquid chromatography (HPLC) (Shimadzu, Kyoto, Japan) was used to quantify α-mangostin in the extracts according to the validated method reported by Yodhnu et al.

Early Version - Uncorrected

(2009)[10]. Total phenolic content was determined using the Folin-Ciocalteu method[11] and expressed as grams of gallic acid equivalents (GAE) per gram of extract. Tannins were quantified using insoluble PVPP, which selectively binds tannins, following the procedure reported by Sultana et al. (2012)[12] and expressed as grams of tannic acid equivalents (TAE) per gram of extract.

Evaluation of the biological activities of mangosteen pericarp extract

Determination of antioxidant activity

Antioxidant activity was evaluated using the DPPH radical scavenging assay according to Pinsuwan et al. (2010)[13]. Briefly, 100 µL DPPH solution (6×10^{-5} M) was mixed with 100 µL of either the sample or the reference standard solution. After incubation at 25 °C for 30 min, the absorbance of the reaction mixture was measured at 517 nm using a microplate reader (PowerWaveX, BioTek, USA). Ascorbic acid was used as the reference standard. DPPH scavenging activity (%) was calculated using Equation (1).

$$\text{DPPH scavenging activity (\%)} = 1 - \frac{\text{Absorbance of in the presence of extract}}{\text{Absorbance in the absence of extract}} \text{x } 100 \quad (1)$$

Antioxidant activity of the extracts was reported as the EC_{50} value, indicating the concentration required to achieve 50% of DPPH radical scavenging.

Assessment of tyrosinase inhibitory activity

The tyrosinase inhibitory activity of the extracts was determined using the dopachrome method following the protocol of Dej-Adisai et al. (2014)[14]. Briefly, 20 µL of mushroom tyrosinase solution (203.3 units/mL) was mixed with phosphate buffer (140 µL, pH 6.8) and 20 µL of either the sample or standard solution. After incubation at 25 °C for 10 min, 20 µL of 0.85 mM L-DOPA was added to initiate the reaction. The optical density (OD) at 492 nm was measured immediately after L-DOPA addition and again after incubation at 25 °C for 20 min using a microplate reader. Kojic acid was used as a standard tyrosinase inhibitor (positive control). The percentage of tyrosinase inhibition was calculated according to Equation (2).

$$\text{Tyrosinase inhibition (\%)} = \frac{A_{control} - A_{sample}}{A_{control}} \text{x } 100 \quad (2)$$

Early Version - Uncorrected

where $A_{control}$ is the difference in OD at 492 nm before and after incubation without the sample, and A_{sample} is the difference in OD in the presence of the sample.

Evaluation of sunscreen activity

Octyl dimethyl para-aminobenzoic acid (PABA) was used as the reference standard for UVB absorption, while oxybenzone was used for broad-spectrum UVA–UVB absorption. The absorbance spectra of samples dissolved in 95% ethanol were recorded between 200 and 400 nm using a UV/Vis spectrophotometer (Spectronic® Genesys™ 5, Milton Roy Company, USA).

The sun protection factor (SPF) of the samples was determined using an Optometrics SPF-290S analyzer (Optometrics Corporation, USA), as previously described by Mingwiman et al. (2016)[15], with some modifications. Briefly, the sample (140 µL) was uniformly spread over a 70 cm² area of Transpore® surgical tape (Nexcare™, 3M, Thailand) to obtain a film thickness of 2 µL/cm². The prepared samples were then exposed to a xenon arc lamp emitting UV radiation in the range of 290–400 nm.

Preparation of α-mangostin-rich extract-loaded liposomes

A modified ethanol injection method was employed to prepare α-mangostin-rich extract-loaded liposomes according to Ungphaiboon et al. (2025)[16]. Different liposomal formulations were developed by varying the extract to phosphatidylcholine weight ratios of 1:1, 1:2, 1:3, 1:4, and 1:5. Formulations exhibiting no precipitation or phase separation were selected for further optimization by incorporating additives, such as Tween 80, chitosan, ethanol, and paraben. The formulation was prepared using two phases: a lipid phase and an aqueous phase. Phosphatidylcholine and α-mangostin-rich extract were dissolved in 95% (v/v) ethanol (10 mL) to form the lipid phase, whereas the aqueous phase consisted of Milli-Q water (10 mL) containing Tween 80. Before mixing, both phases were preheated to 60 °C. Ethanol was removed under reduced pressure using a rotary evaporator at 40 °C. Additives, including chitosan, ethanol, or paraben concentrate, were added to the liposomal dispersion, and the final volume was adjusted to 10 mL using Milli-Q water.

For comparison, liposomal formulations were also prepared using the extract–phospholipid complexation method described by Sandhya et al. (2010)[17]. Potential interactions between the α-mangostin-rich extract and phosphatidylcholine were investigated using Fourier-transform

Early Version - Uncorrected

infrared (FT-IR) spectroscopy. The dried complexes were blended with KBr, and the mixture was compressed into a disc using a hydraulic press at 10 tons. FT-IR spectra were recorded using a Perkin-Elmer Spectrum One spectrophotometer (Germany) across the wavenumber range of 400–4000 cm^{-1} at a resolution of 4 cm^{-1} with 16 scans.

Characterization of liposomes

Particle size, polydispersity index (PDI), and zeta potential were determined by photon correlation spectroscopy (Zetasizer, Malvern Instruments, UK) at 25 °C with a scattering angle of 173°. Liposomal morphology was examined using transmission electron microscopy (JEM-2010, JEOL Ltd., Japan). Entrapment efficiency was evaluated following separation of the non-encapsulated extract by ultracentrifugation at 15,000 rpm and 4 °C for 30 min. After dilution with Milli-Q water (1:1), the α-mangostin content in the supernatant (free fraction) was analyzed. To determine the total α-mangostin content, liposomal vesicles were disrupted with 10% Triton X-100 solution (1:1, v/v). Entrapment efficiency (%) was calculated according to Equation (3).

$$\text{Entrapment efficiency (\%)} = \frac{A_T - A_F}{A_T} \text{x } 100 \qquad (3)$$

where A_T denotes the total α-mangostin content in the liposomal dispersion, while A_F represents the amount of non-entrapped α-mangostin.

Preparation and evaluation of anti-aging formulations

Six lotion base formulations were optimized by adjusting Sepigel® 305 concentrations ranging from 0.5-1.0% (w/v) in distilled water. The formulations were evaluated for cosmetic attributes, such as spreadability, smoothness, and non-greasiness, using a sensory scoring system (0 = not acceptable, 1 = poor, 2 = fair, 3 = good, 4 = excellent). The evaluation involved visual assessment of the formulations following application onto a mirror surface, after which the optimal formulation was selected. The optimized liposomal formulation and free extract were incorporated into the selected lotion base to prepare the anti-aging lotion containing 1.0% w/v α-mangostin-rich extract equivalent to 0.8% w/v α-mangostin. The formulations were visually inspected for physical characteristics such as color, precipitation, and phase separation. The pH and viscosity of the

Early Version - Uncorrected

formulation were measured at 25 °C and 32 °C, respectively, using a pH meter and a Brookfield LVDV-III Ultra rheometer (Brookfield Engineering Laboratories Inc., MA, USA). Bioactive compounds were extracted from the finished products using 10% Triton X-100 (1:1, v/v) prior to bioactivity evaluation, as previously described.

Statistical Analysis

All experiments were performed in three independent replicates. Data are expressed as mean ± standard deviation (S.D.). Data were analyzed using t-test and one-way analysis of variance (ANOVA), with p-value < 0.05 considered statistically significant.

Results

Mangosteen pericarp extracts and bioactive compounds

The crude ethanolic extract of mangosteen pericarp appeared as a dark brown viscous paste, whereas the α-mangostin-rich extract was obtained as a yellow powder (Figure 1). The extraction yields of the ethanolic extract and the α-mangostin-rich extract were 9.0% and 1.1% (w/w), respectively, based on dried mangosteen pericarp.

The contents of α-mangostin, total phenolics, and tannins in the extracts are shown in Table 1. The α-mangostin-rich extract contained 4.4-fold higher α-mangostin content and 1.3–fold higher tannin content than the ethanolic extract. However, no significant differences in total phenolic content were observed between the two extracts. The α-mangostin-rich extract exhibited greater stability than the crude ethanolic extract, retaining 98.5% of α-mangostin after storage at 4 °C for 12 months, compared with 70.7% in the ethanolic extract.

Bioactivities of mangosteen pericarp extract

Antioxidant and tyrosinase inhibitory activities

Both extracts exhibited antioxidant and tyrosinase inhibitory activities. The ethanolic extract demonstrated stronger antioxidant activity than the α-mangostin-rich extract, whereas the

Early Version - Uncorrected

α-mangostin-rich extract showed greater tyrosinase inhibitory activity. However, their activities were lower than those of the reference standards (ascorbic acid and kojic acid, respectively) (Table 2).

Sunscreen activity

UV absorption spectra (Figure 2 (a)) revealed that oxybenzone absorbed across both UVA and UVB regions, confirming its broad-spectrum UV absorption properties. In contrast to oxybenzone, octyl dimethyl PABA, the ethanolic extract, and the α-mangostin-rich extract showed predominant absorption in the UVB region. As shown in Figure 2 (b), the SPF values of octyl dimethyl PABA and the ethanolic extract were independent of concentration; conversely, those of the α-mangostin-rich extract and oxybenzone increased with increasing concentration.

The α-mangostin-rich extract showed lower SPF values than octyl dimethyl PABA at low concentrations but surpassed it at higher concentrations. Moreover, the α-mangostin-rich extract exhibited higher SPF values than both the ethanolic extract and oxybenzone.

Preparation and characterization of liposomes

Based on its strong tyrosinase inhibitory and sunscreen activities, the α-mangostin-rich extract was selected for liposomal encapsulation. Formulations 2-5, 8, 9, 15, and 16 produced homogeneous yellow colloidal dispersions without visible precipitation. These formulations were subsequently evaluated for vesicle size, PDI, zeta potential, and entrapment efficiency (Table 3). Liposomes prepared at extract-to-phospholipid ratios of 1:2–1:4 (formulations 2-4) exhibited vesicle sizes less than 300 nm. Formulations 2 and 3 exhibited relatively high entrapment efficiency and were selected for further modification. Tween 80-containing liposomes (formulations 8 and 9) exhibited high entrapment efficiency but also resulted in larger vesicle sizes. In addition, liposomes containing ethanol (formulation 15) displayed larger vesicles compared with the ethanol-free system (formulation 16).

Based on its small vesicle size and high entrapment efficiency, formulation 16 was identified as the optimal formulation. Transmission electron microscopy revealed spherical, large

Early Version - Uncorrected

unilamellar vesicles (>100 nm) (Figure 3). No significant changes in vesicle size, PDI, zeta potential, or entrapment efficiency were observed after 4 months of storage at 4 °C, confirming the physicochemical stability of the formulation.

FT-IR spectroscopy of liposomal complexes, as indicated in Figure 4, showed spectral shifts indicative of molecular interactions between the extract and phosphatidylcholine. The O–H stretching vibrations of α-mangostin, originally detected at 3421.8 and 3259.0 cm^{-1}, shifted in the complexes, with the band at 3259.0 cm^{-1} no longer present. The ester carbonyl stretching band of phosphatidylcholine shifted from 1739.8 cm^{-1} to 1728.6–1733.8 cm^{-1} upon complex formation, indicating interactions within the hydrophilic regions of the phospholipid bilayer.

Evaluation of anti-aging formulations

Lotion bases formulated with 0.5-1.0% (w/v) Sepigel® 305 exhibited total sensory scores ranging from 4.33 ± 1.39 to 11.67 ± 0.19. Among these, 0.7% (w/v) formulation demonstrated the highest ratings for spreadability, smoothness, and non-greasiness. Based on the optimized lotion base, anti-aging lotions were prepared using 1.0% w/v α-mangostin-rich extract, 0.7% w/v Sepigel® 305 as the thickening agent, and 1.0% w/v paraben concentrate as the preservative.

The anti-aging lotion containing α-mangostin-rich extract–loaded liposomes exhibited a homogeneous milky-yellow appearance (Figure 5), with a pH of 4.87 ± 0.01 and a viscosity of 2542.46 ± 66.14 cP. Compared with the free extract, the liposome-containing lotion exhibited significantly higher SPF and anti-tyrosinase (p-value < 0.05) (Table 2). In contrast, the lotion formulated with free α-mangostin-rich extract displayed poor physical characteristics, forming a non-homogeneous dark-yellow dispersion.

Discussion

Mangosteen pericarp extracts are widely utilized in cosmetic and medicinal applications, particularly for acne and other dermatological conditions. Xanthones, especially α-mangostin, exhibit diverse bioactivities relevant to cosmeceutical applications, including antioxidant[6,18], antibacterial[2,19], anti-tyrosinase[4,19], and sunscreen activities[20,21]. These diverse bioactivities support their potential application as anti-aging ingredients in cosmeceutical formulations.

Early Version - Uncorrected

The findings of this study highlight that extract composition is a key determinant of biological activity. Although both extracts contained comparable levels of total phenolics, the crude ethanolic extract exhibited higher antioxidant activity than the α-mangostin-rich extract, suggesting that antioxidant capacity depends on phytochemical diversity and synergistic interactions rather than total phenolic content alone. These findings are consistent with previous reports demonstrating that the extraction solvent and method markedly affect antioxidant activity[22]. Earlier reports by Weecharangsan et al. (2006)[23] and Pothitirat et al. (2009)[6] also demonstrated that phenolic profile, solvent polarity, and fruit maturity influence radical-scavenging efficacy.

In contrast, enrichment of α-mangostin enhanced tyrosinase inhibitory activity, indicating that α-mangostin is a key antimelanogenic compound. The discrepancy between the IC_{50} obtained in this study and the lower value reported by Tadtong et al. (2009)[19] (67 ng/mL) may be explained by differences in assay conditions, especially enzyme concentration and extraction procedures.

Compared with the crude extract and oxybenzone, the α-mangostin-rich extract showed significantly higher SPF values. The efficient UV absorption of α-mangostin can be attributed to its conjugated polyphenolic structure[24,25], consistent with the high SPF values reported for isolated α-mangostin[20]. Despite a moderate correlation between SPF and total phenolic content, specific structural features appear to have a greater impact than overall antioxidant activity. α-Mangostin also inhibits UVB-induced melanogenesis by modulating microphthalmia-associated transcription factor and oxidative stress pathways[4], highlighting its multifunctional photoprotective potential.

α-Mangostin, a poorly water-soluble compound, was successfully encapsulated within lipid vesicles. The optimized formulation (Liposomes No. 16) exhibited an average vesicle size of approximately 300 nm, indicating its suitability as a nanoscale carrier for topical delivery. The incorporation of bilayer modifiers, including Tween 80 and ethanol, increased entrapment efficiency but enlarged vesicle size, possibly due to reduced interfacial tension and membrane fluidization[13,26]. The optimized formulation achieved a balance between vesicle size and bioactive loading and maintained stability over four months. The liposomal formulations exhibited negative zeta potentials greater than ±30 mV, reflecting sufficient charge for maintaining colloidal stability by preventing aggregation[27]. Charged liposomes may further enhance dermal delivery[28]. FT-IR spectroscopy confirmed that α-mangostin interacts with phosphatidylcholine through hydrogen bonding and hydrophobic interactions, facilitating its incorporation into the lipid bilayer[29]. These

Early Version - Uncorrected

molecular interactions may prevent crystallization and protect the compound against oxidative degradation, thereby improving formulation stability[30].

Incorporating liposomal α-mangostin into the lotion base improved formulation homogeneity and significantly enhanced sunscreen and anti-tyrosinase activities relative to the free extract. Compared with the free extract and the anti-aging lotion containing the encapsulated extract, the lotion base exhibited a lower SPF and lacked antioxidant and anti-tyrosinase activities. This finding aligns with reports that excipients in sunscreen formulations can markedly affect textural characteristics and SPF values[31].

Previous studies have shown that liposomal systems improved dermal penetration of xanthones[32], enhanced barrier function[7], improved bioactive retention[8], and restored inflammatory and matrix markers in irradiated skin[9]. Further in vivo studies are required to validate the efficacy and safety of the present formulation.

Conclusion

Collectively, the results demonstrate that α-mangostin-rich extract possesses multifunctional properties relevant to skin aging, including antioxidant, anti-melanogenic, and UV-protective activities. Liposomal encapsulation significantly resulted in improved physicochemical characteristics and enhanced in vitro biological performance, supporting its potential for further development in cosmeceutical formulations.

Acknowledgment

The authors gratefully acknowledge Pranee Rattanasuwan for her assistance with extract preparation and Dr .Saffanah Mohd Ab Azid for the English language editing of the manuscript.

Funding sources

This research was supported by the Faculty of Pharmaceutical Sciences, Prince of Songkla University, Thailand.

Early Version - Uncorrected

Conflict of interest

The authors declare no conflicts of interest.

References

1. Tobin DJ. Introduction to skin aging. J of Tissue Viability. 2017;26(1):37–46.
2. Amnuaikit T, Phadungkarn T, Wattanapiromsakul C, Boonme P. Formulation development of antibacterial films containing mangosteen peel extract. RJPT 2012;5(8):1058–65.
3. Widowati W, Ginting CN, Lister INE, Girsang E, Amalia A, Wibowo SHB, et al. Anti-aging effects of mangosteen peel extract and its phytochemical compounds: antioxidant activity, enzyme inhibition and molecular docking simulation. Trop Life Sci Res 2020;31(3):127–44.
4. Li X, Zhu X, Wang B, Sun J, Xia Y. α-Mangostin, a safe and natural product as a candidate skin-whitening agent. Sci Rep 2025;16(1):1474.
5. Luangpraditkun K, Kasemkiatsakul P, Sangnim T, Yammen S, Pajoubpong J, Vongsak B. Anti-senescence and anti-photoaging activities of mangosteen pericarp extract on UVA-induced fibroblasts. Cosmetics 2025;12(3).
6. Pothitirat W, Chomnawang MT, Supabphol R, Gritsanapan W. Free radical scavenging and anti-acne activities of mangosteen fruit rind extracts prepared by different extraction methods. Pharm Biol 2010;48(2):182–6.
7. Betz G, Aeppli A, Menshutina N, Leuenberger H. In vivo comparison of various liposome formulations for cosmetic application. Int J Pharm 2005;296(1–2):1–2.
8. Lee MS, Bui HTD, Kim SJ, Lee JB, Yoo HS. Liposome-assisted penetration and antiaging effects of collagen in a 3D skin model. J Cosmet Dermatol 2024;23(1):236–43.
9. Min M, Egli C, Bartolome RA, Sivamani RK. Ex vivo evaluation of a liposome-mediated antioxidant delivery system on markers of skin photoaging and skin penetration. CCID 2024;17:1481–94.
10. Yodhnu S, Sirikatitham A, Wattanapiromsakul C. Validation of LC for the determination of alpha-mangostin in mangosteen peel extract: a tool for quality assessment of Garcinia mangostana L. J Chromatogr Sci 2009;47(3):185–9.

Early Version - Uncorrected

11. Zhang Q, Zhang J, Shen J, Silva A, Dennis DA, Barrow CJ. A simple 96-well microplate method for estimation of total polyphenol content in seaweeds. J Appl Phycol 2006;18(3):445–50.
12. Sultana M, Verma PK, Raina R, Prawez S, Dar MA. Quantitative analysis of total phenolic, flavonoids and tannin contents in acetone and n-hexane extracts of ageratum conyzoides. ChemTech 2012;4(3):996–9.
13. Pinsuwan S, Amnuaikit T, Ungphaiboon S, Itharat A. Liposome-containing *Hibiscus sabdariffa* calyx extract formulations with increased antioxidant activity, improved dermal penetration and reduced dermal toxicity. J Med Assoc Thai 2010;93(Suppl 7):S216-26.
14. Dej-Adisai S, Meechai I, Puripattanavong J, Kummee S. Antityrosinase and antimicrobial activities from Thai medicinal plants. Arch Pharm Res 2014;37(4):4.
15. Muangsiri W. Correlation of in vitro SPF values from two laboratories. TJPS 2016;40 (Suppl):65-8.
16. Ungphaiboon S, Ardhanwanich S, Maneenuan D, Pinsuwan S, Mahasawat P. Evaluation of nano-sized virgin coconut oil (VCO)-loaded liposomes for enhancing mushroom and B16-F10 tyrosinase activity. OpenNano 2025;22:100232.
17. Sandhya S, Chandra SJ, Vinod KR, Rao K, Banji D. Preclinical studies of a novel polyherbal phyto–complex hair growth promoting cream. Asian Pac J Trop Biomed 2012;2(1):S296–304.
18. Rohman, A, Rafi M, Alam G, Muchtaridi M, Windarsih A. Chemical composition and antioxidant studies of underutilized part of mangosteen (*Garcinia mangostana* L.) fruit. J App Pharm Sci 2019;9(8):47–52.
19. Tadtong S, Viriyaroj A, Vorarat S, Nimkulrat S, Suksamrarn S. Antityrosinase and antibacterial activities of mangosteen pericarp extract. J Health Res 2009;23(2):99–102.
20. Liandhajani, Iwo MI, Sukrasno, Soemardji AA, Hanafi M. Sunscreen activity of α -mangostin from the pericarps of Garcinia mangostana. J App Pharm Sci 2013;3,(6):70–3.
21. Im AR, Kim YM, Chin YW, Chae S. Protective effects of compounds from *Garcinia mangostana* L. (mangosteen) against UVB damage in HaCaT cells and hairless mice. Int J Mol Med 2017;40(6):1941–9.
22. Palakawong S, Sophanodora P, Pisuchpen S, Phongpaichit S. Antioxidant and antimicrobial activities of crude extracts from mangosteen (*Garcinia mangostana* L.) parts and some essential oils. IFRJ 2010;17:583–9.

Early Version - Uncorrected

23. Weecharangsan W, Opanasopit P, Sukma M, Ngawhirunpat T, Sotanaphun U, Siripong P. Antioxidative and neuroprotective activities of extracts from the fruit hull of mangosteen (*Garcinia mangostana* Linn.). Med Princ Pract 2006;15(4):281–7.
24. Nichols JA, Katiyar SK. Skin photoprotection by natural polyphenols: anti-inflammatory, antioxidant and DNA repair mechanisms. Arch Dermatol Res 2010;302(2):71–83.
25. Ebrahimzadeh MA, Enayatifard R, Khalili M, Ghaffarloo M, Saeedi M, Yazdani Charati J. Correlation between sun protection factor and antioxidant activity, phenol and flavonoid contents of some medicinal plants. Iran J Pharm Res 2014;13(3):1041–7.
26. Musielak E, Krajka-Kuźniak V. Liposomes and ethosomes: comparative potential in enhancing skin permeability for therapeutic and cosmetic applications. Cosmetics 2024;11(6):191.
27. Kumar A, Badde S, Kamble R, Pokharkar VB. Development and characterization of liposomal drug delivery system for nimesulide. Int J Pharm Pharm Sci 2010;2(4):87–9.
28. Lee MS, Lee JW, Kim SJ, Pham-Nguyen OV, Park J, Park JH, et al. Comparison study of the effects of cationic liposomes on delivery across 3D skin tissue and whitening effects in pigmented 3D skin. Macromol Biosci 2021;21(5):2000413.
29. Aisha AF, Majid AMSA, Ismail Z. Preparation and characterization of nano liposomes of *Orthosiphon stamineus* ethanolic extract in soybean phospholipids. BMC Biotechnol 2014;14(1):23.
30. Yoshida A, Manosroi A, Manosroi J, Yamauchi H, Abe M. Molecular interactions between phospholipids and mangostin in a lipid bilayer. Colloids Surf B Biointerfaces 1995;4(6):423–32.
31. Špaglová M, Čermáková P, Jackuliaková P, Piešťanský J. Role of emulsifiers and SPF booster in sunscreen performance: assessing SPF, rheological behavior, texture, and stability. Cosmetics 2025;12(3):118.
32. Widyanati P, Jufri M, Elya B. Formulation and penetration study of liposome gel xanthone of extract mangosteen pericarp (*Garcinia mangostana* L.). Int J Pharm Sci Rev Res 2014;27(2):1–6.

Early Version - Uncorrected

Table 1 Contents of α-mangostin, tannins, and total phenolics in mangosteen pericarp extracts

Mangosteen pericarp extracts	Bioactive content		
	α-Mangostin (% w/w)	Tannins (mg TEA/g extract)	Total phenolics (mg GAE/g extract)
Crude ethanolic extract	17.8 ± 1.5*	110.6 ± 3.4*	139.1 ± 1.7
α-Mangostin-rich extract	78.7 ± 0.1	142.2 ± 1.7	141.8 ± 1.7

* Significantly different from the α-mangostin-rich extract (p-value < 0.05).

Table 2 In vitro bioactivity of mangosteen pericarp extracts and lotions (mean ± S.D.)

In vitro bioactivity	Antioxidant activity; EC_{50} (μg/mL) (n = 3)	Anti-tyrosinase activity; IC_{50} (μg/mL) (n = 3)	SPF value at 1%w/v (n =6)
Standards and extracts			
- Ascorbic acid	2.56 ± 0.02*	ND	ND
- Kojic acid	ND	3.17 ± 0.34*	ND
- Octyl dimethyl PABA	ND	ND	2.80 ± 0.14*
- Oxybenzone	ND	ND	1.42 ± 0.08*
- Crude ethanolic extract	11.41 ± 0.76*	45.15 ± 0.86*	1.13 ± 0.08*
- α-Mangostin-rich extract	56.78 ± 1.67	29.03 ± 0.75	1.73 ± 0.21
Formulations			
- Lotion base	ND	ND	0.9. ± 0.00*

Early Version - Uncorrected

In vitro bioactivity	Antioxidant activity; EC_{50} (µg/mL) (n = 3)	Anti-tyrosinase activity; IC_{50} (µg/mL) (n = 3)	SPF value at 1%w/v (n =6)
- Lotions containing liposomes No.16	55.38 ± 1.39	17.67 ± 0.42*	3.2 ± 0.10*

* Significantly different from the α-mangostin-rich extract (p-value < 0.05), ND = not determined.

Table 3 Physical characteristics of liposomes containing various compositions

No.	Weight ratio MT:PC:TW80 (Additive)	MT (%w/v)	Vesicle size (nm)	PDI	Zeta potential (mV)	Entrap-ment (%)
1	1:1:0	2.0	ND	ND	ND	ND
2	1:2:0	1.0	224.53 ± 2.04	0.29 ± 0.02	-44.83 ± 1.07	42.6 ± 0.1
3	1:3:0	0.7	212.63 ± 3.20	0.17 ± 0.01	-77.67 ± 4.04	44.5 ± 0.1
4	1:4:0	0.5	275.77 ± 8.43	0.17 ± 0.01	-54.33 ± 2.16	21.1 ± 0.1
5	1:5:0	0.4	224.53 ± 2.04	0.29 ± 0.02	-44.83 ± 1.07	42.6 ± 0.1
6	1:2:0	10.0	ND	ND	ND	ND
7	1:3:0	6.7	ND	ND	ND	ND
8	1:2:0.4	1.0	420.33 ± 6.02	0.28 ± 0.03	-22.47 ± 1.34	76.9 ± 0.1
9	1:2:0.4	2.0	455.27 ± 19.90	0.54 ± 0.05	-80.43 ± 1.72	64.2 ± 0.1
10	1:2:0.4	3.0	ND	ND	ND	ND
11	1:2:0.4	4.0	ND	ND	ND	ND
12	1:2:0.4	5.0	ND	ND	ND	ND

Early Version - Uncorrected

No.	Weight ratio MT:PC:TW80 (Additive)	MT (%w/v)	Vesicle size (nm)	PDI	Zeta potential (mV)	Entrap-ment (%)
13	1:2:0.4 (0.01% w/v CH)	2.0	ND	ND	ND	ND
14	1:2:0.4 (0.005% w/v CH)	2.0	ND	ND	ND	ND
15	1:3:0.6 (15% v/v ET)	1.0	389.87 ± 12.25	0.39 ± 0.01	-19.60 ± 0.87	55.7 ± 1.7
16	1:3:0.6 (1% w/v PB)	1.0	306.83 ± 1.50	0.27 ± 0.01	-38.50 ± 2.49	77.6 ± 0.1

Note: Data are presented as the mean ± S.D. (n = 3). MT = α-mangostrin-rich extract, PC = phosphatidylcholine, TW80 = Tween 80, CH = chitosan, ET = 95% ethanol, PB = paraben concentrate, PDI = polydispersity index, ND = not determined due to precipitation.

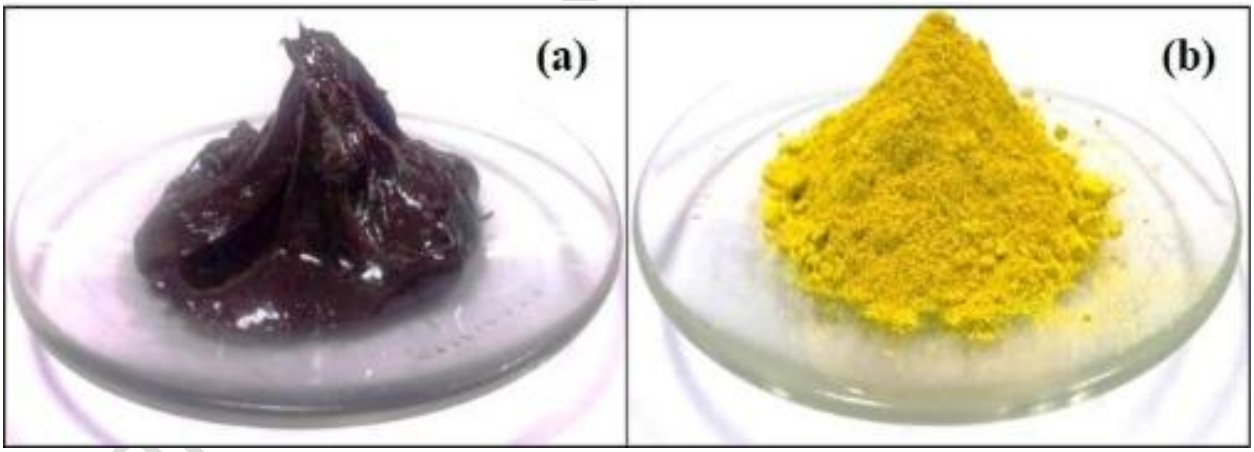


Figure 1 The physical appearance of ethanolic mangosteen extract (a) and α-mangostin-rich extract (b).

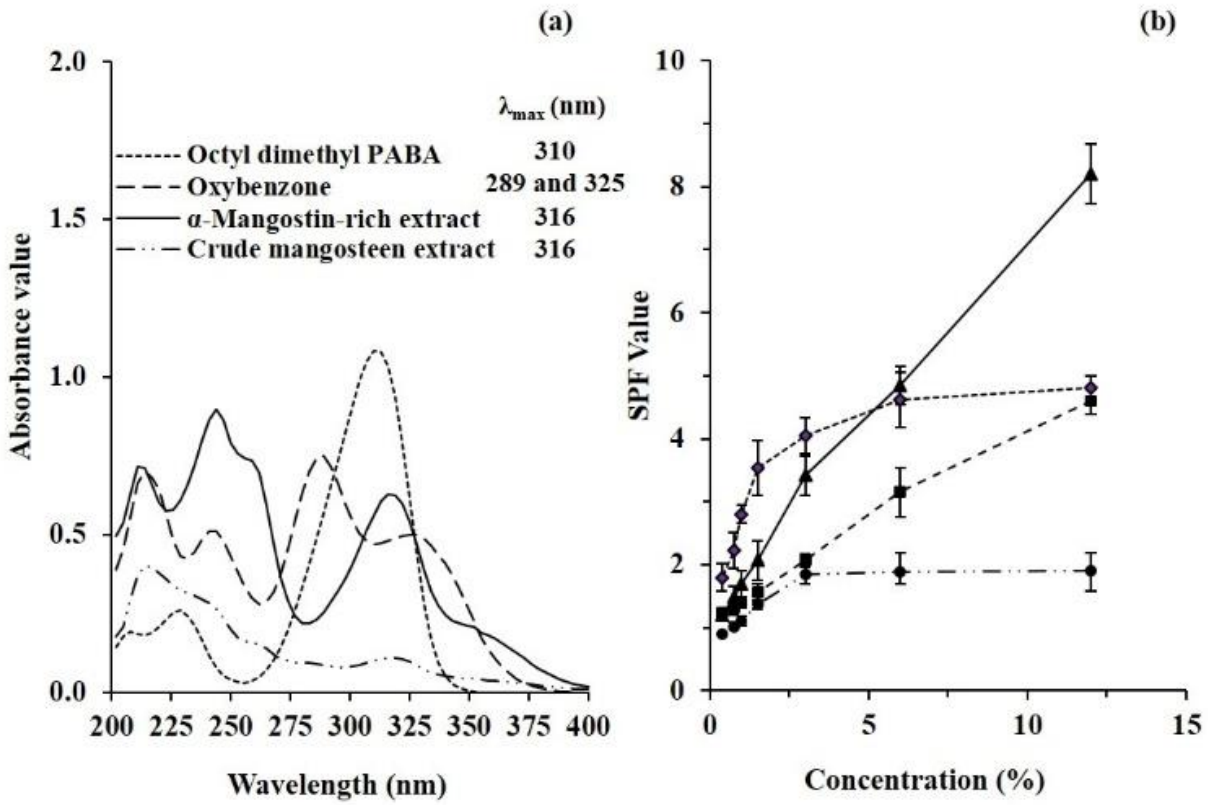


Figure 2 UV absorption spectra of sunscreen chemicals and mangosteen pericarp extracts at 12.5 mg/L (a) and their SPF values determined in 95% v/v ethanol (b).

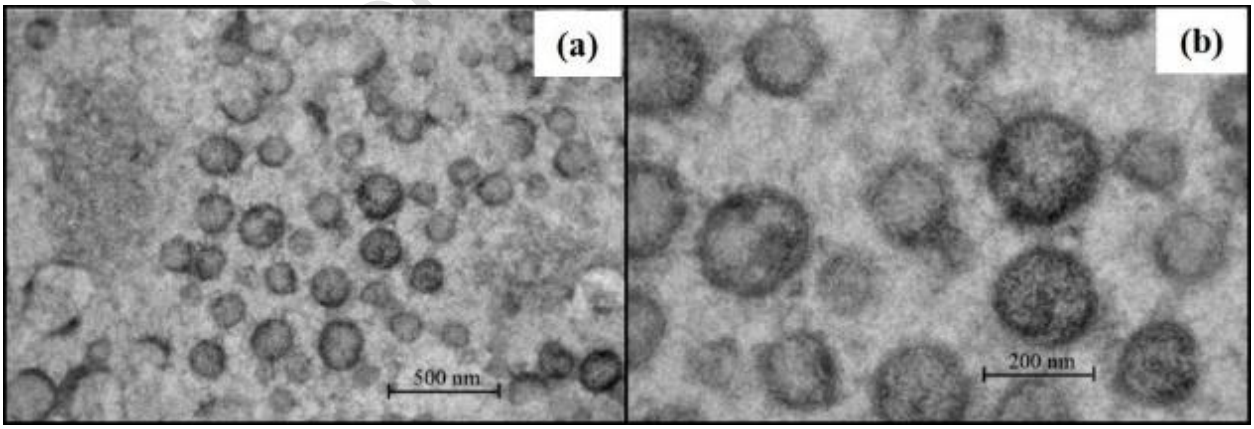


Figure 3 Transmission electron microscope (TEM) images of liposome vesicles from formulation 16 at 20,000x (a) and 50,000x (b).

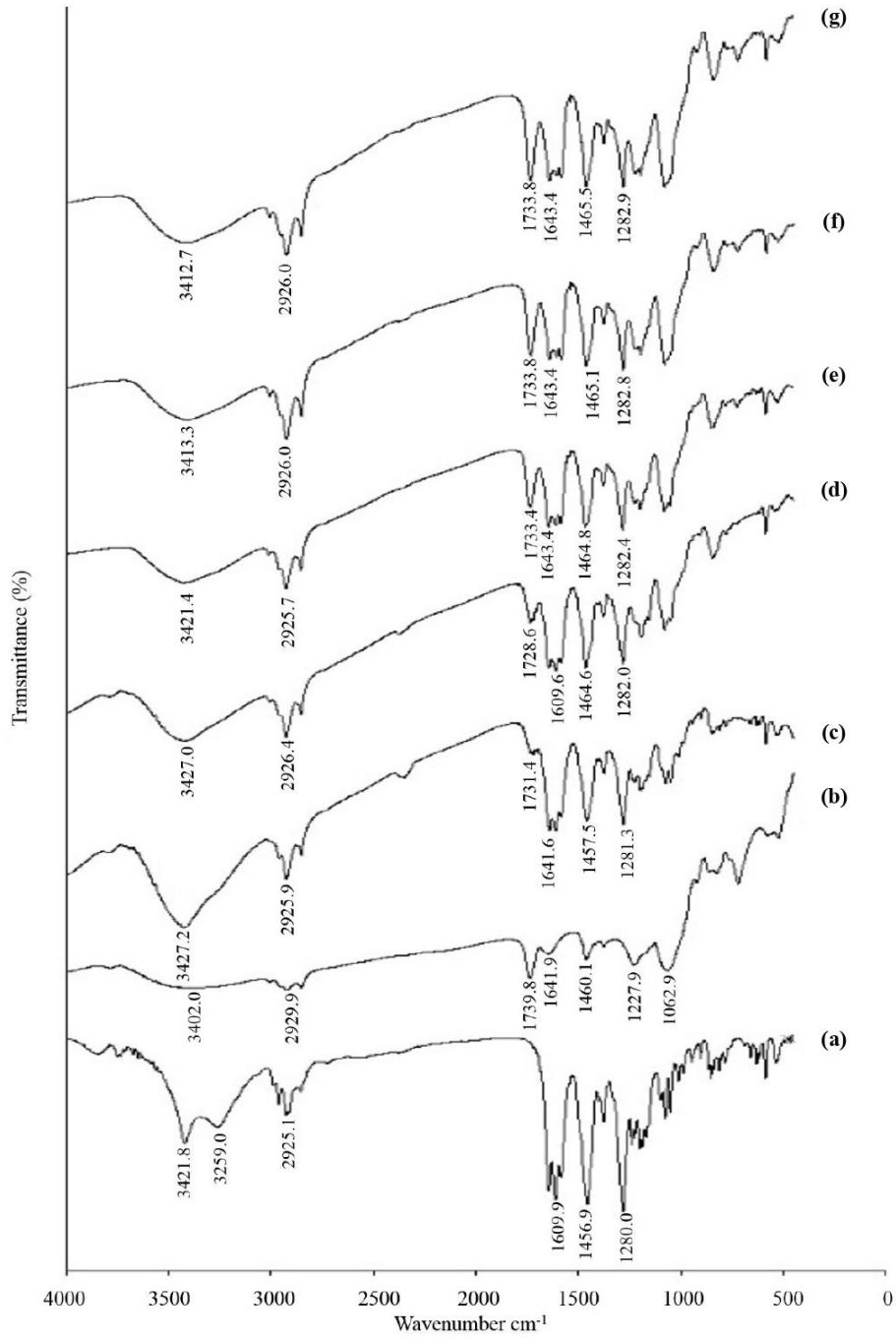


Figure 4 FTIR spectra of α-mangostin-rich extract (a), phosphatidylcholine (b), and α-mangostin-rich extract-phosphatidylcholine complex 1:1 (c), 1:2 (d), 1:3 (e), 1:4 (f), and 1:5 (g).



Figure 5 Appearance of α-mangostin-rich extract-loaded liposomes No. 16 (a), lotion containing liposomes No. 16 (b), and lotion containing the free α-mangostin-rich extract (c).

Early Version